Electronic Supplementary Material (ESI) for Chemical Science.
This journal is © The Royal Society of Chemistry 2018

Electronic Supplementary Information

Shaping excitons in light-harvesting proteins through nanoplasmonics

Stefano Caprasecca,[*,†] Stefano Corni,[*,‡,¶] and Benedetta Mennucci[*,†]

†*Dipartimento di Chimica e Chimica Industriale, Università di Pisa, I-56124 Pisa, Italy*

‡*Dipartimento di Scienze Chimiche, Università di Padova, I-35131 Padova, Italy*

¶*Istituto Nanoscienze, Consiglio Nazionale delle Ricerche CNR-NANO, I-41125 Modena, Italy*

E-mail: stefano.caprasecca@for.unipi.it; stefano.corni@unipd.it; benedetta.mennucci@unipi.it

1 Supplementary Discussion

1.1 Extrinsic effect on degenerate states

Figure S1 reports the contributions to the effective molecular dipole moment for states S2 and S3, in the presence of the resonant NT-850 particle. In general, the imaginary contribution of the metal is larger than the real one, as it is to be expected close to the plasmonic resonance, see Figure 1 E (main text).

The dipole moment induced on the metal contributes to S3 nearly nine times as much as to S2. To rationalize such behavior, the dipoles induced on the metal by each localized transition are individually represented in Figure S1, weighted by the relative coefficient. The exciton dipoles are obtained by weighing each local dipole by its corresponding exciton coefficient, the latter being those already perturbed by the intrinsic effect of the metal. The different signs and magnitudes of the coefficients are therefore responsible for the combination of localized dipoles, which is particularly favorable in the S3 case, where all the localized dipoles (bar few negligible exceptions) combine constructively. This is not so in the case of S2, where several large dipole moments cancel out. This is due to the fact that $\boldsymbol{\mu}_{\mathrm{met}}^{\mathrm{tr}}$ are virtually all along the same direction, which is the polarization axis of the metal, and the signs of the coefficients play the major role by combining them constructively or destructively. The effect here illustrated for NT-850 is observed for other nanotips and nanorods as well.

1.2 Effect of disorder

Figure S2 shows the effect of disorder on the spectra and populations, obtained after irradiation at two different energy ranges.

In the top panel, NT-850 is used, and the sample is irradiated at the low-energy end of the spectrum. The population localization observed in the crystal structure remains almost unperturbed when disorder is accounted for. The spectrum on the right shows that the absorption of the low-energy states is enhanced. The three peaks correspond to states S3,

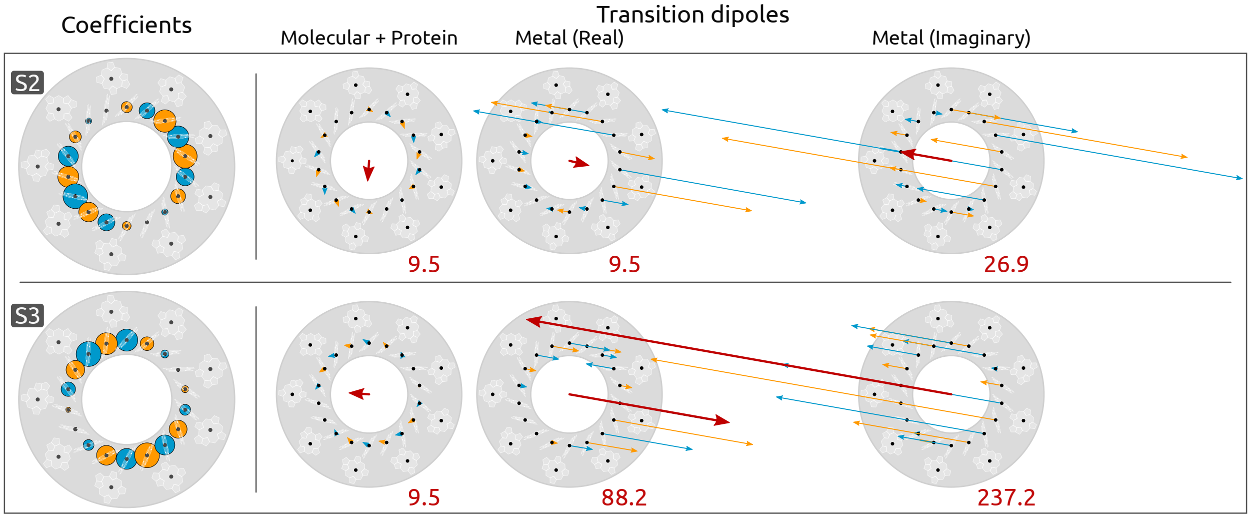

Figure S1: Exciton states S2 and S3 in the presence of NT-850. Left: exciton coefficients, including the implicit metal effect, represented by circles placed on the BChl units. Right: Molecular transition dipoles and dipoles induced on the protein environment and the metal nanoparticle (both real and imaginary parts). The dipoles are represented as vectors applied to the BChls that induce them. The red arrows represent the resulting exciton transition dipole moments (on a different scale), with norm explicitly indicated in red.

S5 and S7, delocalized over the B850 ring. Note that there is a marked oscillator strength redistribution, causing the three peaks to be significantly wider than the B800 ones at high energy, owing to the large coupling in the B850 ring.

In the bottom panel, NT-800 is used, and the sample is irradiated at the high-energy end of the spectrum. The population localization observed in the crystal structure remains almost unperturbed when disorder is accounted for. The spectrum on the right shows that the absorption of the high-energy states is enhanced, and the low-energy ones are several orders of magnitude smaller. The highest peak corresponds to state S22, while oscillator strength redistribution over the other B800 states at high energy is also observed.

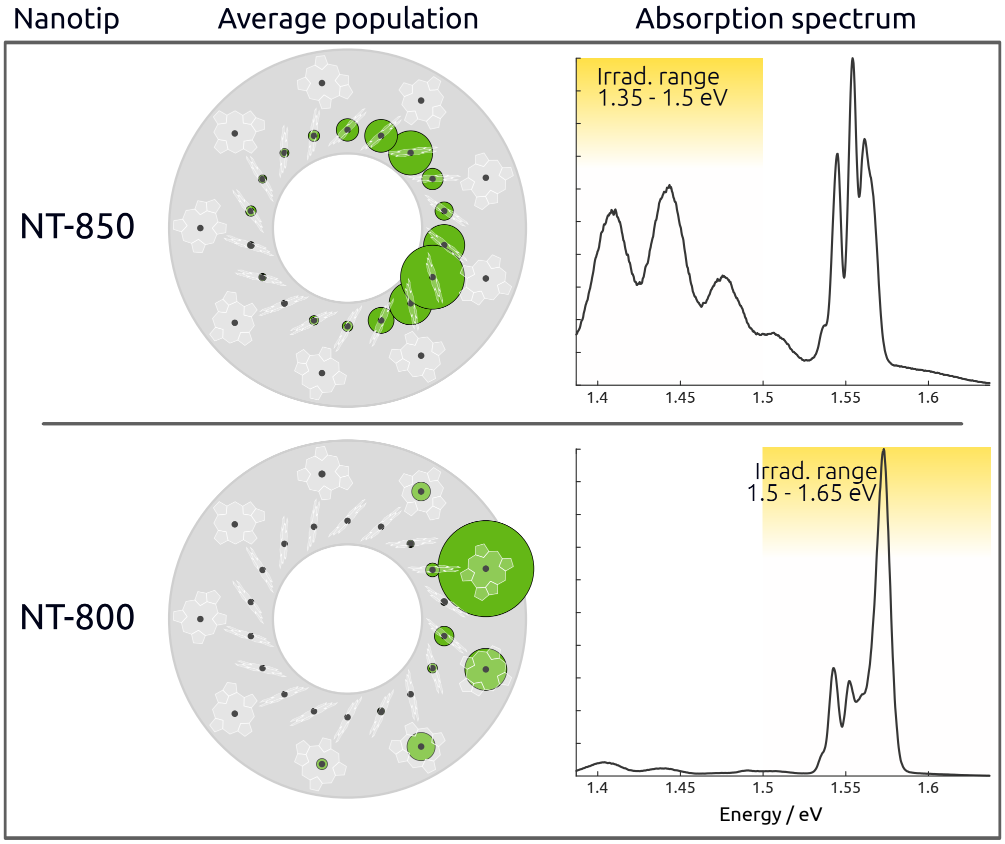

Figure S2: Left: average population of each BChl under the irradiation of light polarized along the main NT axis in two energy ranges (top: 1.35 – 1.5 eV, bottom: 1.5 – 1.65 eV) over 100,000 realizations obtained by including a diagonal static disorder. Right: Average absorption spectrum over the realizations including static disorder, obtained using Lorentzian lineshapes with 5 cm^{-1} homogeneous broadening. The LH2 system is perturbed by NT-850 (top) and NT-800 (bottom), and the irradiation is considered in the low- and high-energy regions of the spectrum, respectively, where the NTs are resonant. Significant contributions to the average population: for NT-850 BChls β_9 (31%), β_2 (15%), α_9 (14%), α_1 (13%); average PR: 6.1. For NT-800 BChls γ_1 (69%), γ_9 (13%); average PR: 2.0.

2 Supplementary Tables

Table S1: Transition energies (in eV), character of the exciton states and participation ratio (PR) in the symmetric unperturbed LH2.

	State	Comp. Energy	Character	PR
1	B850, $k = 0$	1.39	Dark	17.8
2	B850, $k = \pm 1$	1.41	Bright	11.8
3		1.41	Bright	11.8
4	B850, $k = \pm 2$	1.44	Dark	11.6
5		1.44	Dark	11.6
6	B850, $k = \pm 3$	1.48	Dark	10.8
7		1.48	Dark	10.7
8	B850, $k = \pm 4$	1.50	Dark	7.8
9		1.50	Dark	7.8
10	B800, $k = 0$	1.54	Quasi-dark	9.0
11	B800, $k = \pm 1$	1.54	Bright	6.0
12		1.54	Bright	6.0
13	B850, $k = \pm 5$	1.55	Dark	7.8
14		1.55	Dark	7.8
15	B800, $k = \pm 2$	1.55	Dark	6.0
16		1.55	Dark	6.0
17	B800, $k = \pm 3$	1.56	Dark	6.0
18		1.56	Dark	6.0
19	B850, $k = \pm 6$	1.56	Dark	10.8
20		1.56	Dark	10.9
21	B800, $k = \pm 4$	1.56	Dark	6.0
22		1.56	Dark	6.0
23	B850, $k = \pm 7$	1.58	Dark	11.5
24		1.58	Dark	11.5
25	B850, $k = \pm 8$	1.59	Quasi-dark	11.7
26		1.59	Quasi-dark	11.7
27	B850, $k = 9$	1.59	Quasi-dark	17.8

Table S2: Exciton energies (E), in eV, and their variation induced by the MNPs (Δ), in cm^{-1}. The new ordering of states after the shift is indicated in parenthesis when applicable.

			Δ			
	State	E	NT-800		NT-850	
1	B850, $k = 0$	1.39	-1		5	
2	B850, $k = \pm 1$	1.41	-4		2	
3		1.41	0		29	
4	B850, $k = \pm 2$	1.44	-3		0	
5		1.44	0		20	
6	B850, $k = \pm 3$	1.48	0		14	(7)
7		1.48	-1		-6	(6)
8	B850, $k = \pm 4$	1.50	0		0	
9		1.50	1		0	
10	B800, $k = 0$	1.54	6		0	
11	B800, $k = \pm 1$	1.54	4		0	
12		1.54	20	(14)	2	
13	B850, $k = \pm 5$	1.55	0	(12)	0	
14		1.55	2	(13)	1	
15	B800, $k = \pm 2$	1.55	1		0	
16		1.55	26		2	
17	B800, $k = \pm 3$	1.56	0		0	(18)
18		1.56	18	(19)	0	(17)
19	B850, $k = \pm 6$	1.56	1	(18)	1	
20		1.56	0		0	
21	B800, $k = \pm 4$	1.56	0		0	
22		1.56	60		0	
23	B850, $k = \pm 7$	1.58	0		1	
24		1.58	0		0	
25	B850, $k = \pm 8$	1.59	0		0	
26		1.59	0		0	
27	B850, $k = 9$	1.59	0		0	

Table S3: Exciton squared dipole moments ($|\boldsymbol{\mu}|^2$), in au^2, and their variation induced by the MNPs (Δ).

			Δ	
	State	$\|\boldsymbol{\mu}\|^2$	NT-800	NT-850
1	B850, $k = 0$	0.0	0.0	0.1
2	B850, $k = \pm1$	92.4	-0.1	-0.1
3		92.4	0.0	-1.2
4	B850, $k = \pm2$	0.0	0.1	0.0
5		0.0	0.0	0.9
6	B850, $k = \pm3$	0.0	0.0	0.1
7		0.0	0.0	0.0
8	B850, $k = \pm4$	0.0	0.0	0.0
9		0.0	0.0	0.0
10	B800, $k = 0$	1.6	1.5	0.0
11	B800, $k = \pm1$	49.6	-1.6	0.0
12		49.6	-6.2	-0.1
13	B850, $k = \pm5$	0.0	0.0	0.0
14		0.0	0.0	0.0
15	B800, $k = \pm2$	0.0	0.3	0.0
16		0.0	2.2	0.0
17	B800, $k = \pm3$	0.0	0.0	0.0
18		0.0	0.5	0.0
19	B850, $k = \pm6$	0.0	0.0	0.0
20		0.0	0.0	0.0
21	B800, $k = \pm4$	0.0	0.0	0.0
22		0.0	3.6	0.0
23	B850, $k = \pm7$	0.0	0.0	0.0
24		0.0	0.0	0.0
25	B850, $k = \pm8$	0.8	0.0	0.0
26		0.8	0.0	0.0
27	B850, $k = 9$	2.4	0.0	0.0

Table S4: Exciton participation ratio (PR) and their variation induced by the MNPs (Δ).

	State	PR	Δ	
			NT-800	NT-850
1	B850, $k = 0$	17.8	0.0	-0.1
2	B850, $k = \pm 1$	11.8	0.1	0.0
3		11.8	0.0	-0.3
4	B850, $k = \pm 2$	11.6	0.0	0.0
5		11.6	0.0	0.3
6	B850, $k = \pm 3$	10.8	0.0	-0.1
7		10.7	0.0	0.2
8	B850, $k = \pm 4$	7.8	0.3	0.1
9		7.8	0.3	0.1
10	B800, $k = 0$	9.0	-0.4	0.0
11	B800, $k = \pm 1$	6.0	0.1	0.0
12		6.0	-0.8	0.0
13	B850, $k = \pm 5$	7.8	0.0	0.0
14		7.8	0.0	0.0
15	B800, $k = \pm 2$	6.0	0.0	0.1
16		6.0	-0.9	0.1
17	B800, $k = \pm 3$	6.0	0.1	0.3
18		6.0	-0.3	0.3
19	B850, $k = \pm 6$	10.8	0.0	0.0
20		10.9	0.0	0.0
21	B800, $k = \pm 4$	6.0	0.0	0.9
22		6.0	-4.2	0.8
23	B850, $k = \pm 7$	11.5	0.1	0.5
24		11.5	0.1	0.5
25	B850, $k = \pm 8$	11.7	0.1	0.2
26		11.7	0.1	0.2
27	B850, $k = 9$	17.8	0.0	0.0

3 Supplementary Figures

3.1 Nanotip geometry

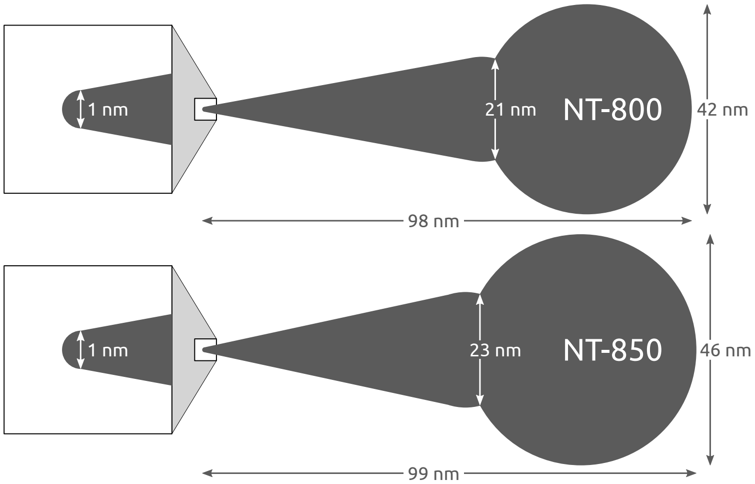

Figure S3: Geometry of the tips considered. The dimensions are indicated. The sphere connected to the metal tip has been introduced to avoid the (artificial) localized plasmonic excitations arising because of the tip truncation. Moreover, this shape is also more representative of effective picocavity-forming metal tip.

3.2 Unperturbed system

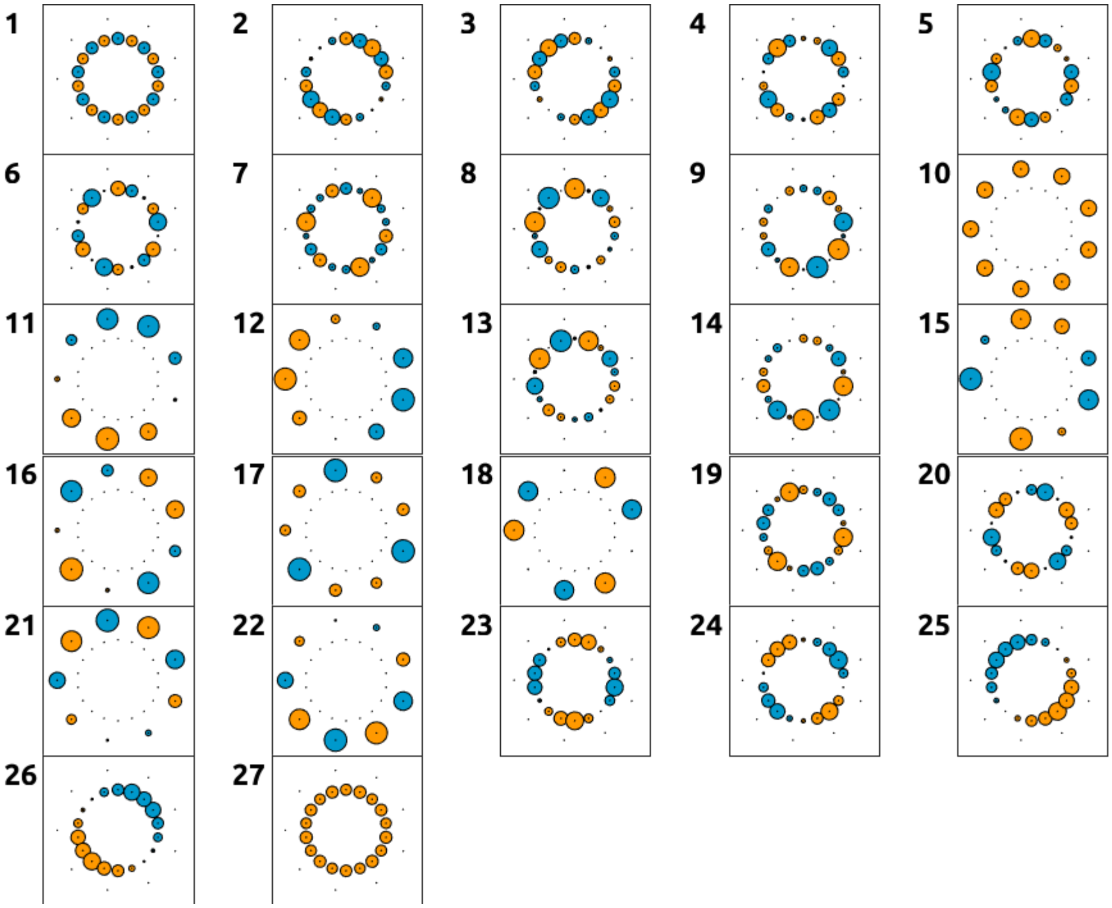

Figure S4: Unperturbed exciton coefficients. Circles are placed on each of the BChl units m, having radius proportional to $|C_{Mm}|$ and therefore areas proportional to $|C_{Mm}|^2$. The numbers identify the exciton states. The signs are indicated using different colors.

3.3 Nanotip NT-800

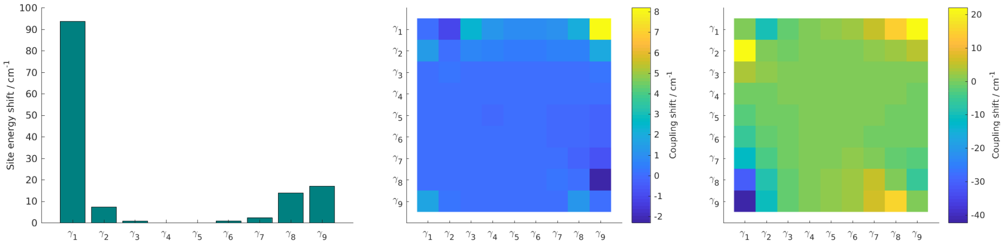

Figure S5: Perturbation induced by NT-800 on B800 BChl site energies and couplings, in cm^{-1}. Left panel: shifts of site energies. Mid panel: shifts of couplings (below diagonal: Coulomb couplings; above diagonal: protein environment-induced couplings). Right panel: metal-induced coupling terms (below diagonal: real component; above diagonal: imaginary component).

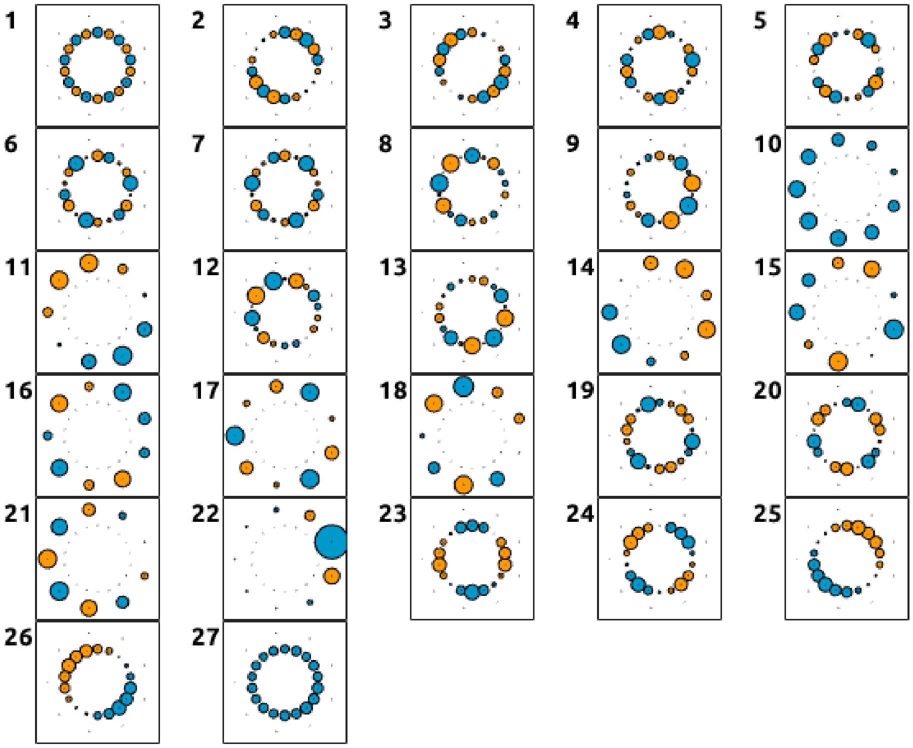

Figure S6: Exciton coefficients perturbed by NT-800. Circles are placed on each of the BChl units m, having radius proportional to $|C_{Mm}|$ and therefore areas proportional to $|C_{Mm}|^2$. The numbers identify the exciton states. The signs are indicated using different colors.

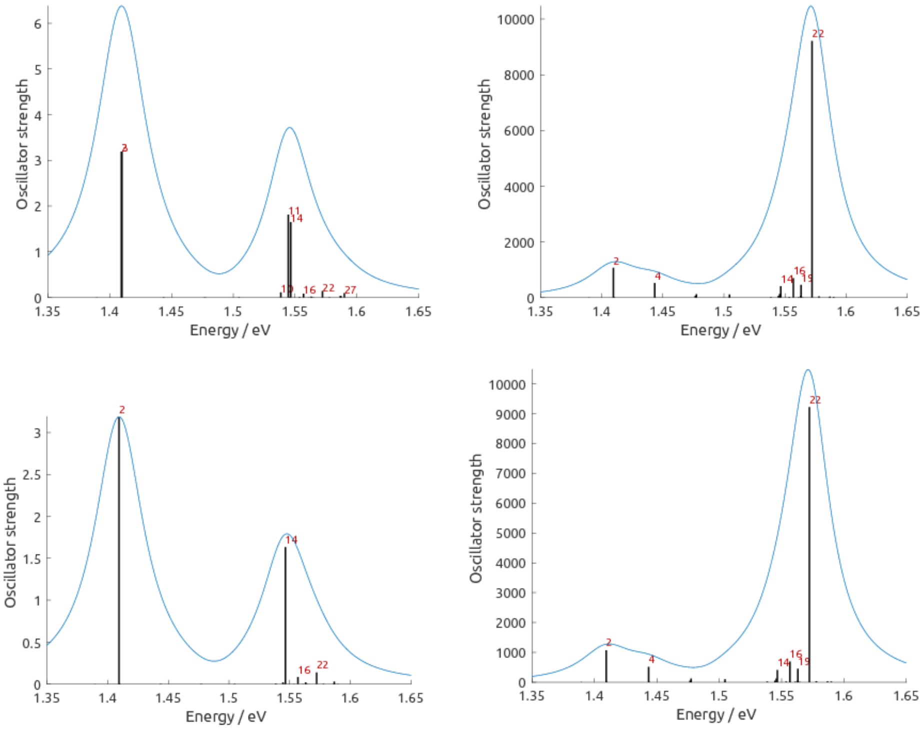

Figure S7: Simulated absorption spectra with NT-800. Top: unpolarized light. Bottom: light polarized along NT axis. Left: intrinsic effect only. Right: both intrinsic and extrinsic effects. The spectra including intrinsic+extrinsic effects appear almost identical when polarized (bottom) and unpolarized (top) light is used. In fact, due to the amplification of the light electric field along the nanotip axis direction, the spectra are dominated by transitions with dipole along such direction, and polarized vs unpolarized lights end up giving the same results. This is to be contrasted with the left panels, where only intrinsic effects are considered, which means that the amplification and the effective polarization in the local electric field due to the tip is disregarded. Here, transitions with a dipole perpendicular to the tip axis can be excited, the spectra are thus richer in features that moreover show a polarization dependence.

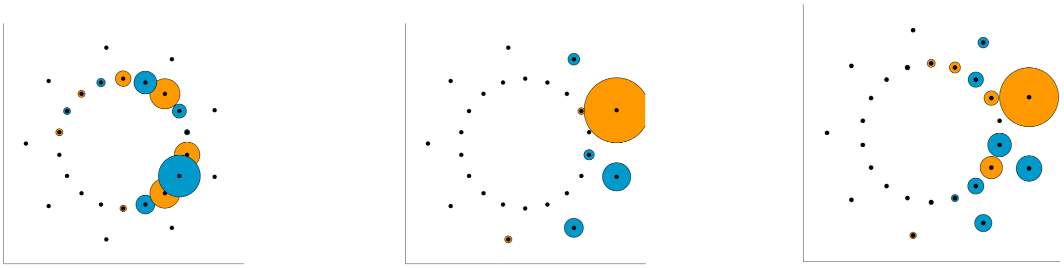

Figure S8: Superposition excited by light polarized along the NT-800 main axis. Left: irradiation range 1.35 – 1.5 eV. PR: 6.0. Exciton states involved: S2 (40%), S4 (28%). BChls: α_1 (11%), β_2 (16%), α_9 (15%), β_9 (30%). Mid: irradiation range 1.5 – 1.65 eV. PR: 1.8. Exciton states involved: S22 (40%). BChls: γ_1 (73%), γ_9 (14%). Right: irradiation range 1.35 – 1.65 eV, PR: 3.3. Exciton states involved: S22 (26%). BChls: γ_1 (52%), γ_9 (10%).

3.4 Nanotip NT-850

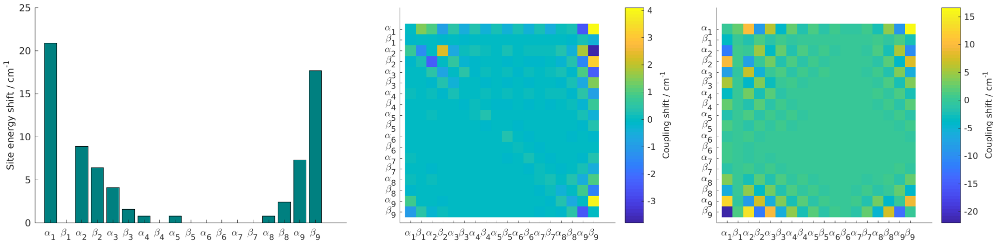

Figure S9: Perturbation induced by NT-850 on B850 BChl site energies and couplings, in cm^{-1}. Left panel: shifts of site energies. Mid panel: shifts of couplings (below diagonal: Coulomb couplings; above diagonal: protein environment-induced couplings). Right panel: metal-induced coupling terms (below diagonal: real component; above diagonal: imaginary component).

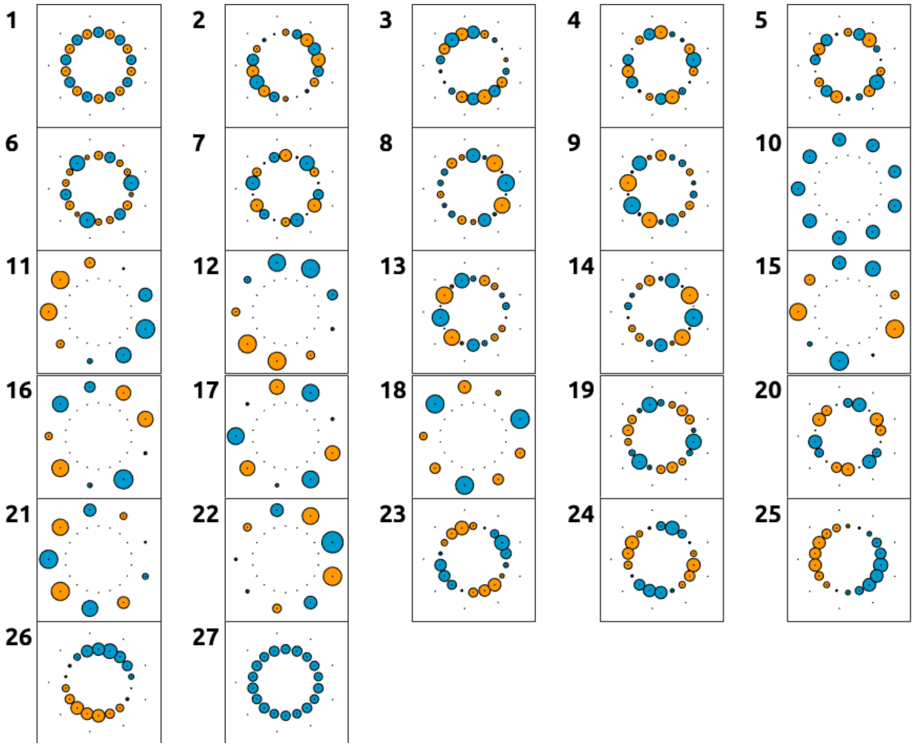

Figure S10: Exciton coefficients perturbed by NT-850. Circles are placed on each of the BChl units m, having radius proportional to $|C_{Mm}|$ and therefore areas proportional to $|C_{Mm}|^2$. The numbers identify the exciton states. The signs are indicated using different colors.

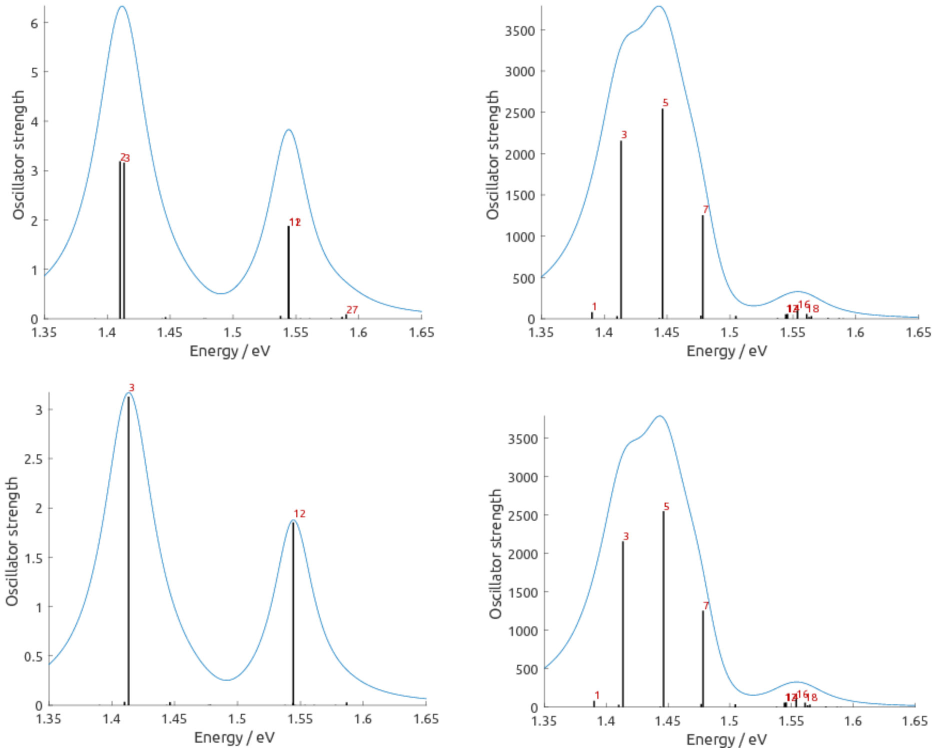

Figure S11: Simulated absorption spectra with NT-850. Top: unpolarized light. Bottom: light polarized along NT axis. Left: intrinsic effect only. Right: both intrinsic and extrinsic effects. The considerations done for Figure S7 apply also here. Note in particular that using unpolarized light allows to excite states S2 (dipole perpendicular to tip axis) and S3 (dipole parallel to tip axis) when only intrinsic effects are considered (top-left). On the contrary, only S3 can be excited when intrinsic+extrinsic effects are considered, independently from the use of unpolarized (top-right) or polarized (bottom-right) light, due to the local tip-enhanced field.

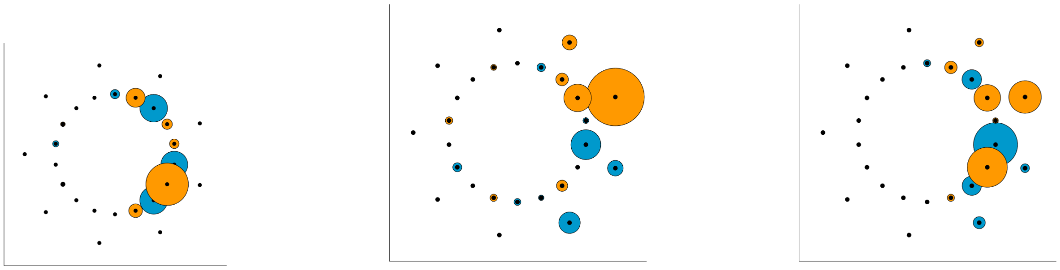

Figure S12: Superposition excited by light polarized along the NT-850 main axis. Left: Irradiation range 1.35 – 1.5 eV, PR: 4.9, exciton states involved: S3 (30%), S5 (32%), S7 (22%). BChls: α_1 (14%), β_2 (15%), α_9 (15%), β_9 (36%). Mid: Irradiation range 1.5 – 1.65 eV, PR: 3.5, exciton states involved: S9, S12, S14, S16, S18, S22 (<15%). BChls: α_1 (13%), γ_1 (50%), α_2 (11%). Right: Irradiation range 1.35 – 1.65 eV, PR: 5.4, exciton states involved: S3, S5, S7, S16 (<15%). BChls: α_1 (29%), γ_1 (16%), α_2 (11%), β_9 (24%).